

## Natural convection in a cavity filled with nanofluids

Abd el Malik Bouchoucha, Rachid Bessaïh

Laboratoire d'Énergétique Appliquée et de Pollution Département de Génie mécanique, Faculté des Sciences de la Technologie. Université Frères Mentouri – Constantine 1. Route de Ain El Bey, 25000 Constantine, Algérie

[bouchoucha.malik@gmail.com](mailto:bouchoucha.malik@gmail.com)

**Abstract**— The present paper deals with a numerical study of natural convection in a cavity filled with nanofluids. The highest temperature value stands for the left vertical wall,  $T_h$  (heat source), the right vertical wall is kept at a low temperature,  $T_c$  and the other walls are isolated. The equations of continuity, Navier-Stokes and energy were solved by using the finite-volume method based on the SIMPLER algorithm. A computer program was developed and compared with the numerical results found in the literature. Results were presented in terms of streamlines, isotherms, local and average Nusselt numbers for the Rayleigh number ( $10^3 \leq Ra \leq 10^6$ ), solid volume fraction of nanoparticles ( $0 \leq \phi \leq 0.10$ ), dimensionless length of the heat source ( $B=0.5$ ), and the type of nanofluids (Cu, Ag,  $Al_2O_3$  and  $TiO_2$ ). The results show that the previous parameters have considerable effects on the flow and thermal fields.

**Keywords**— Natural convection, Nanofluid, Cavity.

### Nomenclature

$B$	dimensionless heat source length		
$C_p$	specific heat, $J\ kg^{-1}\ K^{-1}$	$\alpha$	thermal diffusivity, $m^2\ s^{-1}$
$k$	thermal conductivity, $Wm^{-1}\ K^{-1}$	$\beta$	thermal expansion coefficient, $K^{-1}$
$L$	cavity length, m	$\phi$	solid volume fraction
$Nu_s$	local Nusselt number along the heat source	$\theta$	dimensionless temperature

$Nu_m$	average Nusselt number	$\mu$	dynamic viscosity, $\text{kg m}^{-1}\text{s}^{-1}$
$U, V$	dimensionless velocity components	$\nu$	kinematic viscosity, $\text{m}^2\text{s}^{-1}$
$X, y$	Cartesian coordinates, m	$\rho$	density, $\text{kg m}^{-3}$
$X, Y$	dimensionless coordinates ( $x/L, y/L$ )	$\psi$	dimensionless stream function
$P$	dimensionless pressure	H	hot
$g$	gravitational acceleration, $\text{ms}^{-2}$	$P$	nanoparticle
		$f$	fluid (pure water)

## 1. Introduction

Nano-scale particle added fluids are called as nano-fluid, this technique was introduced by Choi [1]. Compared with the suspended particles of millimetres or higher, nanofluids have greater stability and rheological properties, higher thermal conductivity and negligible pressure drop. Nano-fluids seem to constitute a very interesting alternative for electronic cooling applications, micro-electromechanical systems, process heating and cooling to energy conversion and supply and magnet cooling, etc.

During the several past years, numerical studies of nanofluid free convection in a square cavity were well studied and discussed [2-6]. Aminossadati and Ghasemi [7] investigated numerical study of free convection of nanofluid in a square cavity cooled from two vertical and top horizontal walls and heated by a constant heat flux heater on its horizontal bottom wall. It was found that type of nanoparticles and the length and location of the heat source affected significantly the heat source maximum temperature. Khanafer et al. [8] investigated the heat transfer enhancement in a two-dimensional enclosure utilizing nanofluids for various pertinent parameters. They tested different models for nanofluid density, viscosity, and thermal expansion coefficients. It was found that the suspended nanoparticles substantially increase the heat transfer rate any given Grashof number. Koblinski et al. [9] found that the increase of nanofluids thermal conductivity is due to the Brownian motion of particles, the molecular-level layering of the liquid at the liquid/particle interface, the nature of heat transport in the nanoparticles, and the effect of nanoparticle clustering. Saleh et al. [10] investigated numerically heat transfer enhancement of nanofluid in a trapezoidal enclosure using Water–Cu and water–Al<sub>2</sub>O<sub>3</sub>, and developed a correlation of the average Nusselt number as a function of the angle of the sloping wall, effective thermal conductivity and viscosity as well as Grashof number. Cheng [11-13] studied a diversity of free convection such as non-Newtonian nanofluids about a vertical truncated cone in a porous medium, where he illustrated that increasing the thermophoresis parameter or the Brownian motion parameter tends to reduce the Nusselt number. Chou et al. [14] studied natural convection heat transfer performance in a complex-wavy-wall enclosed. The accomplished work confirms that the presented results in of this study provide a useful insight into the natural convection heat transfer of nanofluids. Oztop et al. [15] numerically analysed the problem of steady state natural convection in an enclosure filled with a nanofluid by using heating and cooling sinusoidal temperature profiles on one side. They found that the addition of nanoparticles into water affects the fluid flow and temperature distribution especially for higher Rayleigh numbers. Mahmoudi et al. [16] investigated the problem of free convection fluid flow and heat transfer of Cu–water nanofluid inside a square cavity having adiabatic square bodies at its centre. The results show that for all Rayleigh numbers with the exception of  $Ra = 10^4$ , the average Nusselt number increases with an increase in the volume fraction of the nanoparticles. Jou and Tzeng [17] used nanofluids to enhance natural convection heat transfer in a two-dimensional rectangular enclosure for various parameters. They conducted a numerical study using Khanafer's model. They indicated that the solid volume fraction of nanofluids causes an increase in the average heat transfer coefficient.

The objective of this study is to investigate the steady laminar natural convection in a square cavity filled with nanofluid. The influence of relevant parameters such as the Rayleigh number, solid volume fraction, type of nanofluids on flow and thermal fields and on local and average Nusselt numbers were studied. This geometry has potential application in the cooling of electronic components.

## 2. Mathematical formulation and numerical model

### 2.1 Problem description

The configuration considered in this study is shown in figure 1. The fluid in the cavity is a water based nanofluid containing Copper nanoparticles. The left vertical wall is kept at a local hot temperature  $T_H$ , the right vertical wall is maintained at a local cold temperature  $T_C$ , and the remaining boundaries are adiabatic. The base fluid (water) used is incompressible, Newtonian fluid that satisfies the Boussinesq hypothesis, and the nanofluid is assumed to be incompressible and the flow is laminar. The thermo-physical properties of the nanofluid are constant, except for the variation of density, which is estimated by the Boussinesq hypothesis.

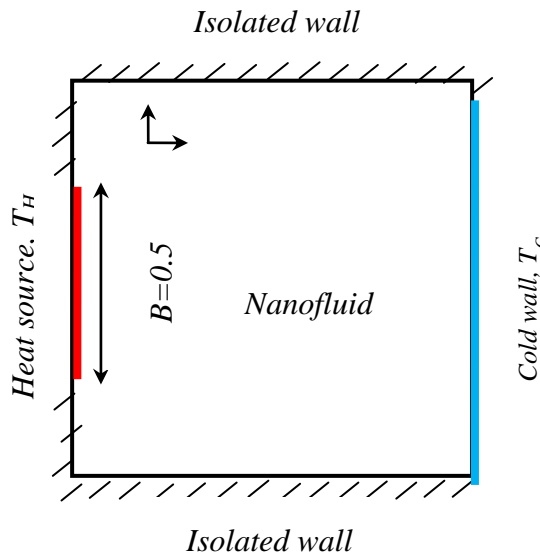


Fig. 1. A schematic diagram of the physical model.

### 2.2. Governing Equations

The continuity, momentum and energy equations for the laminar and steady state natural convection in the two-dimensional cavity can be written in dimensional form as f

$$\frac{\partial u}{\partial x} + \frac{\partial v}{\partial y} = 0 \quad (1)$$

$$u \frac{\partial u}{\partial x} + v \frac{\partial u}{\partial y} = \frac{1}{\rho_{nf}} \left[ -\frac{\partial p}{\partial x} + \mu_{nf} \left( \frac{\partial^2 u}{\partial x^2} + \frac{\partial^2 u}{\partial y^2} \right) \right] \quad (2)$$

$$u \frac{\partial v}{\partial x} + v \frac{\partial v}{\partial y} = \frac{1}{\rho_{nf}} \left[ \frac{\partial p}{\partial y} + \mu_{nf} \left( \frac{\partial^2 v}{\partial x^2} + \frac{\partial^2 v}{\partial y^2} \right) + (\rho\beta)_{nf} g(T - T_c) \right] \quad (3)$$

$$u \frac{\partial T}{\partial x} + v \frac{\partial T}{\partial y} = \alpha_{nf} \left( \frac{\partial^2 T}{\partial x^2} + \frac{\partial^2 T}{\partial y^2} \right) \quad (4)$$

The effective density of the nanofluid is given as:

$$\rho_{nf} = (1 - \phi)\rho_f + \phi\rho_p \quad (5)$$

where  $\phi$  is the solid volume fraction of nanoparticles.

The thermal diffusivity of the nanofluid is

$$\alpha_{nf} = k_{nf} / (\rho C_p)_{nf} \quad (6)$$

where, the heat capacitance of the nanofluid is given by:

$$(\rho C_p)_{nf} = (1 - \phi) (\rho C_p)_f + \phi (\rho C_p)_p \quad (7)$$

The thermal expansion coefficient of the nanofluid can be determined by

$$(\rho\beta)_{nf} = (1 - \phi) (\rho\beta)_f + \phi (\rho\beta)_p \quad (8)$$

The effective dynamic viscosity of the nanofluid given by Brinkman [18] is:

$$\mu_{nf} = \frac{\mu_f}{(1 - \phi)^{2.5}} \quad (9)$$

In Equation (2),  $k_{nf}$  is the thermal conductivity of the nanofluid, which for spherical nanoparticles, according to Maxwell [19] is:

$$k_{nf} = \left[ \frac{(k_p + 2k_f) - 2\phi(k_f - k_p)}{(k_p + 2k_f) - \phi(k_f - k_p)} \right] \quad (10)$$

In order to cast the governing equations into a dimensionless form, the following dimensionless parameters are introduced:

$$X = \frac{x}{L}, Y = \frac{y}{L}, U = \frac{uL}{\alpha_f}, V = \frac{vL}{\alpha_f}, P = \frac{\bar{p}L^2}{\rho_{nf}\alpha_f^2}$$

$$\theta = \frac{T - T_c}{\Delta T (= T_h - T_c)}, Ra = \frac{g\beta_f L^3 \Delta T}{\nu_f \alpha_f}, Pr = \frac{\nu_f}{\alpha_f}$$

The non-dimensional continuity, momentum and energy equations are written as follows:

$$\frac{\partial U}{\partial X} + \frac{\partial V}{\partial Y} = 0 \quad (11)$$

$$U \frac{\partial U}{\partial X} + V \frac{\partial U}{\partial Y} = -\frac{\partial P}{\partial X} + \frac{\mu_{nf}}{\rho_{nf}\alpha_f} \left( \frac{\partial^2 U}{\partial X^2} + \frac{\partial^2 U}{\partial Y^2} \right) \quad (12)$$

$$U \frac{\partial V}{\partial X} + V \frac{\partial V}{\partial Y} = -\frac{\partial P}{\partial Y} + \frac{\mu_{nf}}{\rho_{nf}\alpha_f} \left( \frac{\partial^2 V}{\partial X^2} + \frac{\partial^2 V}{\partial Y^2} \right) + \frac{(\rho\beta)_{nf}}{\rho_{nf}\beta_{nf}} Ra Pr \theta \quad (13)$$

$$U \frac{\partial \theta}{\partial X} + V \frac{\partial \theta}{\partial Y} = \frac{\alpha_{nf}}{\alpha_f} \left( \frac{\partial^2 \theta}{\partial X^2} + \frac{\partial^2 \theta}{\partial Y^2} \right) \quad (14)$$

### 2.3. Boundary Conditions

The dimensionless boundary conditions are:

$$U = 0, \quad V = 0, \quad \theta = 1, \quad X = 0, \quad 0 \leq Y \leq 1$$

$$U = 0, \quad V = 0, \quad \theta = 0, \quad X = 1, \quad 0 \leq Y \leq 1$$

$$U = 0, \quad V = 0, \quad \frac{\partial \theta}{\partial X} = 0, \quad Y = 0, \quad 0 \leq X \leq 1$$

$$U = 0, \quad V = 0, \quad \frac{\partial \theta}{\partial X} = 0, \quad Y = 1, \quad 0 \leq X \leq 1$$

### 3. Numerical method and code validation

The governing equations presented in Eqs. (11)- (14) along with the boundary conditions were solved by using FORTRAN code, which using a control volume formulation [25]. The numerical procedure called SIMPLER [25] was used to handle the pressure-velocity coupling. For treatment of the convection and diffusion terms in equations (12)-(14), the power-law and central difference schemes were adopted. The convergence was obtained when the energy balance between the heat source and the cold wall is less than a prescribed accuracy value, i.e., 0.1%.

#### 3.1. Code validation

With the numerical results of Aminossadati and Ghasemi [7] at  $Ra=10^5$ ,  $\phi=0$  and 0.10 for the local Nusselt number  $Nu$  (Fig.2a) and the dimensionless temperature  $\theta_s$  along the heat source (Fig.2b). As shown in Figures 2a-b, it is clear that our results are in good agreement with the numerical results of references [7].

#### 3.2. Grid Independence Study

The study was undertaken to six grids: 122×122, 132×132, 142×142, 152×152 and 162×162, 172×172 nodes. Table 2 shows the variation of the maximum values  $Nu_m$  with grid size for Cu-water nanofluid,  $B=1$ ,  $\phi = 0.1$  and  $Ra=10^5$ . The changes in the calculated values are very small for three 152×152, 162×162, 172×172 grids and we noticed that the variation of  $Nu_m$  between 152×152 and 162×162 nodes is less than 0.001248 (Table 2). However, and after running tests of independence between the numerical solution and the mesh, the fourth grid 152×152 nodes was chosen to complete the calculations. This grid also gives the best compromise between cost and accuracy of calculations.

Table 1. Grid independency results (Cu-water nanofluid,  $B=1$ ,  $\phi = 0.1$ , and  $Ra=10^5$ )

Grid	122×122	132×132	142×142	152×152	162×162	172×172
$Nu_m$	5.251923	5.250128	5.248814	5.247566	5.246435	5.248814

#### 4. Results and discussion

Figure 3 represents the variation of the average Nusselt number ratio as a function of the nanoparticles volume fraction and for heat source length  $B=0.5$ , for various values of the Rayleigh number. We show that the average Nusselt number is independent of the  $Ra < 10^3$ . In this case, we note the improved average Nusselt number with the increasing the volume fraction of nanoparticles. This is due to the enhancement of the effective thermal conductivity of the nanofluid with the increasing of the volume of nanoparticles. It is found that the addition of nanoparticles to a significantly improve in the average Nusselt number, and the heat transfer inside the cavity is dominated by conduction regime effect. In addition, the effect of the nanoparticles is more significant in the low Rayleigh number than the high Rayleigh number. For ( $10^3 < Ra < 10^4$ ), the average Nusselt number increases in a non-linear way with the increasing of Rayleigh number because the heat transfer is associated to conduction and convection regime effect. For  $Ra > 10^4$ , the average Nusselt number increases linearly with the increase of Rayleigh number, this is justified by the high buoyancy force effects, and the heat transfer inside the cavity is dominated by convection. Also, the highest values for Nusselt number are found at  $Ra = 10^6$ , where a stronger buoyant flow field appears in the enclosure. The figure shows that the Nusselt numbers are starting from the same value. It is worth to remark that, the Rayleigh number values move away according to the solid volume increasing.

Figure 4 shows the variation of the average Nusselt number ratio as a function of the nanoparticles volume fraction, for various values of the Rayleigh number. We show that the average Nusselt number ratio increases almost monotonically with increasing concentration for all nanofluids, and this increase is negligible for small values of number of  $Ra$  (the natural convection mode). For high values of the Rayleigh number ( $Ra=10^5$ ), we find the increase in the average Nusselt number ratio with the augmentation of the nanoparticles volume fraction, and this is justified by the increased of heat transfer mode by convection. Also, we see that the average Nusselt ratio decreases as a function of the nanoparticle type (Ag, Cu,  $Al_2O_3$ ,  $TiO_2$ ) and the lowest value of the average Nusselt ratio was obtained for  $TiO_2$  nanoparticles, this can be justified by the effect of the heat transfer mode by conduction and their low thermal conductivity compared to the other type of nanoparticle. However, the difference between the values of the average Nusselt ratio of Ag and Cu is negligible; this is due to the thermal conductivity effect of the nanoparticle type as it has shown in table (1). In addition, we show that the average Nusselt number of the Ag and Cu nanoparticle are similar. We conclude that the highest value of the average Nusselt ratio is obtained for the type Ag nanoparticle.

Figure 5 shows the local Nusselt number profile concerned the nanofluid at  $Ra= 10^5$ , for different solid volume fraction values. We notice that the local Nusselt number takes highest solid volume fraction values that fact leads to its increasing. Therefore, the local Nusselt number increasing is depending to the solid volume fraction increasing.

Figure 6 shows the vertical velocity profile along the mid-section of the enclosure, one can notice that, the velocity profiles are inversed, which indicate the flow rotation direction. It is worth to remark that, the flow rises on the left side and descends near the vertical wall. It is also obviously clear that the absolute vertical velocity magnitude increases with the maximum temperature. In addition, the velocity increases according to the solid volume fraction increasing.

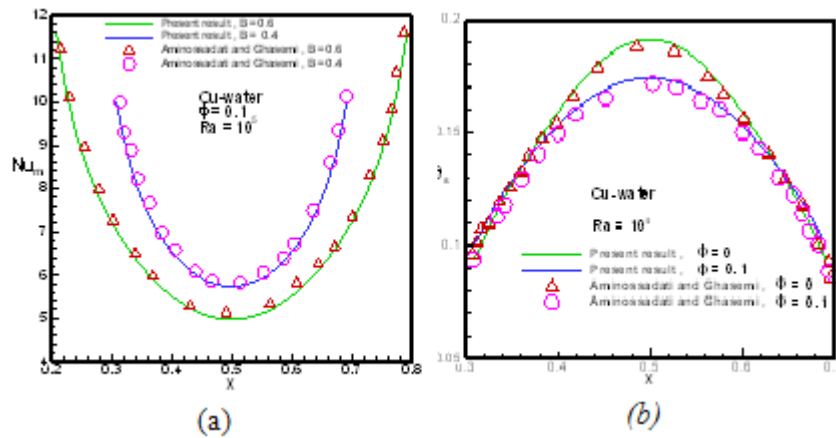


Fig. 2 .Comparison between our results and those of Aminossadati and Ghasemi [7] at  $Ra=10^5$ ,  $\phi=0$  and 0.10: (a) Local Nusselt number  $Nu$  and (b) dimensionless temperature  $\theta_s$  along the heat source.

Figure 7 presents velocity profile along the vertical median of the enclosure for  $Ra= 105$ , and different volume fraction. Figure 7 shows a symmetric flow for a median plane of the enclosure. The flow velocity along the middle of the enclosure is equal to zero when the heat source is located to the left wall. The circulating cell on the left side of the enclosure becomes limited as the heat source moves towards the left side of the bottom wall. As a consequence, the right circulating cell grows and moves towards the centre of the enclosure. The velocity in the enclosure axis for the highest value of the Rayleigh number is very small compared to the limits levels ones where the fluid is moving with high velocities. This behaviour presents a single-phase flow. As the volume fraction increases, the velocity components of nanofluid increase as a consequence of an increase in the energy transport during the fluid. High velocity peaks of the vertical velocity component are illustrated in this figure at high volume fractions, when the heat source moves towards the middle the maximum velocity increases significantly increases, the velocity components of nanofluid increase as a consequence of an increase in the energy transport during the fluid. High velocity peaks of the vertical velocity component are illustrated in this figure at high volume fractions, when the heat source moves towards the middle the maximum velocity increases significantly.

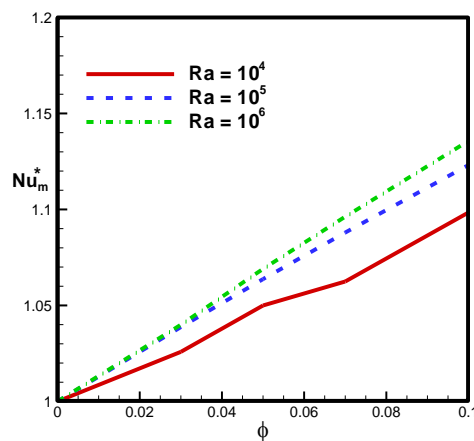


Fig.3.Variation of average Nusselt number ratio with solid volume fraction  $\phi$  at various Rayleigh numbers .



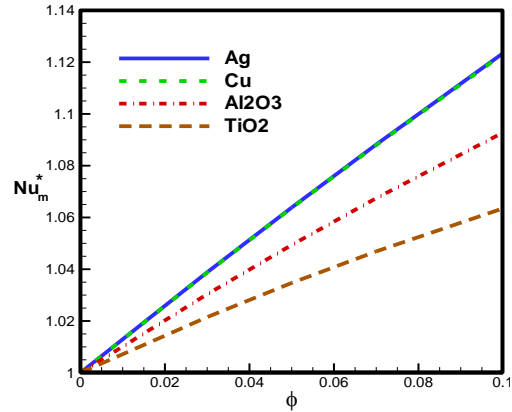


Fig.4.Variation of average Nusselt number ratio with solid volume fraction  $\phi$  for dimensional heat source length  $B=0.5$ , at  $Ra=10^5$  and various nanofluids.

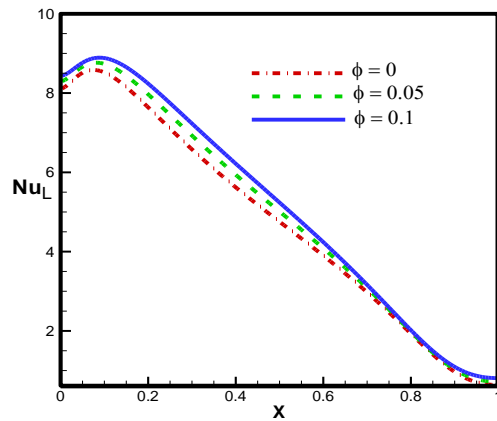


Fig.5. Profile of local Nusselt number  $Nu_L$  along the heat source for various solid volume fractions  $\phi$  at  $Ra=10^5$  and Cu–water nanofluid.

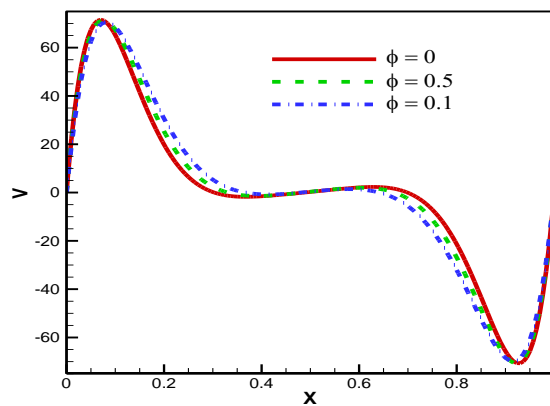


Fig. 6 Vertical velocity profiles  $V$  at  $Y=0.50$  for various solid volume fractions  $\phi$  at  $Ra=10^5$  and Cu–water nanofluid.

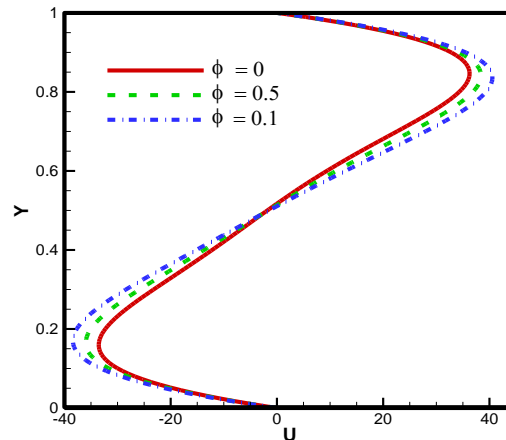


Fig. 7. Horizontal velocity profiles  $U$  at  $X=0.50$  for various solid volume fractions  $\phi$  at  $Ra=10^5$  and Cu–water nanofluid.

## 5. Conclusion

The important concluding remarks are presented:

- The effect of nanofluid on natural convection is particularly evident for high Rayleigh numbers.
- The nanoparticles when immersed in a fluid are capable of increasing the heat transfer capacity of base fluid. As solid volume fraction increases, and the effect is more pronounced.
- The type of nanofluid is a key factor for heat transfer enhancement. The highest values are obtained when using Cu nanoparticles.

## References

- [1] Aminossadati, S.M, and Ghasemi, B., Enhanced Natural Convection in an Isosceles Triangular Enclosure Filled with a Nanofluid, *Computers and Mathematics with Applications*, 61(2011) 1739–1753.
- [2] Ho, C.J., Chen, M.W., and Li.,Z.W, Numerical Simulation of Natural Convection of Nanofluid in a Square Enclosure: Effects Due to Uncertainties of Viscosity and Thermal Conductivity, *International Journal of Heat and Mass Transfer*, 51 (2008), 4506–4516.
- [3] Mahmoodi, M., and Sebdani, S.M., 2012, Natural Convection in a Square Cavity Containing a Nanofluid and an Adiabatic Square Block at the Center, *Superlattices and Microstructures*, 52 (2012) 261–275.
- [4] Jmai, R., Ben-Beya, B., and Lili, T, Heat Transfer and Fluid Flow of Nanofluid-Filled Enclosure with Two Partially Heated Side Walls and Different Nanoparticles,” *Superlattices and Microstructures* .53 (2013) 130–154.
- [5] Ho, C.J., Chen, M.W., and Li.,Z.W, Numerical Simulation of Natural Convection of Nanofluid in a Square Enclosure: Effects Due to Uncertainties of Viscosity and Thermal Conductivity, *International Journal of Heat and Mass Transfer*, 51 (2008) 4506–4516.
- [6] Ooi, E.H., and Popov, V Numerical Study of Influence of Nanoparticle Shape on the Natural Convection in Cu-water Nanofluid, *International Journal of Thermal Sciences*, 65 (2013), 178-188.
- [7] S.M. Aminossadati, B. Ghasemi Natural convection cooling of a localised heat source at the bottom of a nanofluid-filled enclosure. *European Journal of Mechanics B/Fluids* 28 (2009). 630–640.
- [8] K. Khanafer, K. Vafai, M. Lightstone, Buoyancy- driven heat transfer enhance-ment in a two- dimensional enclosure utilizing nanofluid-filled. *European Journal of Mechanics B/Fluids* 28 (2009). 630–640.

- [9] Keblinski, S.R.,Phillpot, S.U.S Choi, J.A.Eastman. Mechanism of heat flow in suspensions of nano-sized particles (nanofluides). *International Journal of Heat and Mass Transfer* 45 (2002) 855-863.
- [10] H. Saleh, R. Roslan, I. Hashim. Natural convection heat transfer in a nanofluid-filled trapezoidal enclosure. *International Journal of Heat and Mass Transfer* 45(2002) 855-863.
- [11] Cheng, C.Y, Free Convection of Non-Newtonian Nanofluids About a Vertical Truncated Cone in a Porous Medium," *International Communications in Heat and Mass Transfer*,39 (2012) 1348–1353.
- [12] Cheng, C.Y Free Convection Boundary Layer Flow Over a Horizontal Cylinder of Elliptic Cross Section in Porous Media Saturated by a Nanofluid, *International Communications in Heat and Mass Transfer* ,39 (2012) 931–936.
- [13] Cheng,C.Y, Natural Convection Boundary Layer Flow Over a Truncated Cone in a Porous Medium Saturated by a Nanofluid, *International Communications in Heat and Mass Transfer* ,39( 2012). 231–235.
- [14] Cho, C.C., Chen,C-L., and Chen, C.,2012,Natural Convection Heat Transfer Performance in Complex-Wavy-Wall Enclosed Cavity Filled with Nanofluid, *International Journal of Thermal Sciences*, 60.(2012) 255-263.
- [15]Oztop, H., Abu-Nada,E., Varol,Y., and Al-Salem, K. ,Computational Analysis of Non-Isothermal Temperature Distribution on Natural Convection in Nanofluid Filled Enclosures, *Superlattices and Microstructures* ,49 (2011). 453–467.
- [16] Mahmoodi, M., and Sebdani, M., Natural Convection in a Square Cavity Containing a Nanofluid and an Adiabatic Square Block at the Center,*Superlattices and Microstructures*, 52, (2012) 261–275.
- [17] Jou,R.Y., and Tzeng, S.C,Numerical Research of Natural Convective Heat Transfer Enhancement Filled with Nanofluids in Rectangular Enclosures,"*International Communications in Heat and Mass Transfer*, 33.(2006) 727–736.
- [18] H.C. Brinkman, The viscosity of concentrated suspensions and solution, *J. Chem. Phys.*20 (1952) 571-581.
- [19] J. Maxwell, *A Treatise on Electricity and Magnetism*, second ed. Oxford University Press, Cambridge, UK, 1904.